Superconducting Nb-Ta-Al-AlOx-Al
Tunnel Junctions for X-Ray Detection

M. C. Gaidis, S. Friedrich, D.E. Prober, A.E. Szymkowiak*, and S.H. Moseley*

Department of Applied Physics, Yale University, New Haven, CT 06520-2157
* NASA Goddard Space Flight Center, Greenbelt, MD 20771

We report progress on the microlithographic fabrication of Nb-Ta-Al-AlOx-Al structures designed for x-ray detection. These structures use bandgap engineering both for quasiparticle trapping to increase the collection efficiency and to prevent quasiparticle diffusion out through the leads. Non-standard tunnel junction geometries are used to reduce the magnetic field needed to suppress the Josephson current for stable biasing. The performance of these devices as alpha particle detectors is presented.

1. INTRODUCTION

Improved x-ray detectors exhibiting single photon efficiency and very good energy resolution ($\Delta E/E \approx 10^{-3}$) will provide answers to many fundamental questions in particle physics and astrophysics. We are concerned primarily with the development of cryogenic detectors for x-ray astronomy applications. Such detectors in satellites like NASA's AXAF will observe K-shell x-rays in the range 100 eV to 8 keV. One of the more promising detector schemes, superconducting tunnel junctions (STJs) exhibit the single photon efficiency needed for faint celestial sources while potentially offering the energy resolution necessary for determination of atomic ionization structure, source velocity structure, and plasma temperatures, densities, and elemental abundances.

Approximately 1000 times more charge carriers are produced by x-rays absorbed in STJs than by those absorbed in semiconducting p-n junction detectors, leading to a projected factor of ≈ 30 better energy resolution. STJs may also be preferable to cryogenic calorimeter detectors because of faster response times, greater design flexibility, and potentially higher operating temperature. The theoretical[1] and experimental[2] feasibility of STJs as x-ray detectors has been demonstrated, yet further advances must be made before a robust detector is available which fulfills theoretical performance expectations.

2. DEVICE DESIGN AND FABRICATION

Important considerations for the x-ray absorbing thin film include energy gap size, thermal cyclability, x-ray absorption depth, quasiparticle (qp) recombination time,

and qp diffusion length. Tantalum is arguably the best material to use, although only preliminary studies of Ta have explored its experimental applicability.[3]   The tunnel junction used for qp detection should also meet some stringent requirements: low subgap current and low capacitance for low electronic noise, stability upon thermal cycling, and compatibility with standard thin film photolithography techniques. Al-Al Oxide-Al tunnel junctions can fulfill these requirements, and are widely used in this application. The choice of an Al base electrode and a Ta x-ray absorber allows the use of qp trapping[4] for improved qp collection efficiency. Quasiparticle trapping is also used in our devices to inhibit qp diffusion out the leads. Contact to the Ta absorber is made with niobium; its high gap should effectively eliminate this qp loss mechanism.
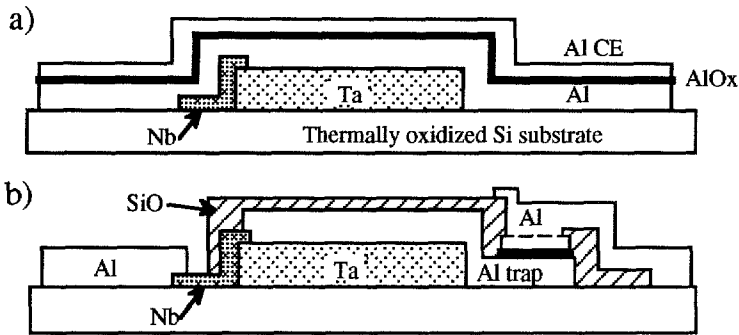
Figure 1: Fabrication of STJ X-ray Detectors (side view)
a. Al-AlOx-Al trilayer deposited over Ta absorber and Nb contact
b. SiO protective coating and Al wiring form the completed device

The fabrication of the STJ x-ray detectors is outlined in Figure 1. Tantalum absorber deposition takes place first, with 5000Å sputter deposited on thermally oxidized Si. A 3000Å amorphous SiO_2 surface layer on the substrate prevents x-ray induced ballistic substrate phonons from registering large signals in the tunnel junctions. The Ta is deposited at 650°C with 10^{-8} torr background pressure. These parameters result in films with the desired bcc Ta phase rather than the low-T_c beta phase.[5] Previously, a thin Nb underlayer had been used to nucleate the bcc phase, but concern over unwanted trapping by metallic Nb suboxides at the substrate interface led us to eliminate this layer. The present deposition procedure results in Ta with $T_c \approx 4.3$ K and a residual resistance ratio (RRR) of $R_{300K}/R_{10K} \approx 16$. This is very good film quality for a non-epitaxial film, and should give us a sufficiently long diffusion length to ensure good charge collection, and reduced qp self-recombination (hotspot) effects. The Ta absorber dimensions of 100 μm x 200 μm are defined by SF_6 RIE, rather than a $FeCl_3$ wet etch as used previously, to prevent the possible incorporation of Fe precipitates in the Ta surface.

The Nb contact layer is deposited next, sputtered to a thickness of ≈1250Å. For good contact between the Nb and Ta, the Ta surface is ion beam cleaned *in situ* just prior to the Nb deposition. The Nb wiring features are defined with a $CF_4 + O_2$ RIE, adjusted for minimal Ta etching. We subsequently ion beam clean the entire wafer *in situ* and

immediately deposit the Al-AlOx-Al trilayer. The ≈ 2000Å thick Al base electrode is thermally evaporated at >200Å/s for best film purity and long diffusion length (the intrinsic RRR of ≈ 30 is reduced to ≈ 10 only because of surface scattering). We oxidize to form the tunnel barrier in 500 mtorr of pure O_2 for 2 hours, then evaporate the ≈ 800Å Al counterelectrode (CE) at a relatively slow 20Å/s to prevent barrier damage. The Al qp trap is defined by a 50°C phosphoric acid etch (PAE), and a more controllable room temperature PAE etch is used for junction area definition. The junction area is approximately 1700 μm^2, with capacitance ≈ 85 pF, less than that of the cables. Approximately 1000Å of thermally evaporated SiO provides junction isolation and a protective coating. It is patterned by photoresist liftoff. The final step is another ion beam cleaning followed by thermal evaporation of a 3000Å Al wiring layer.

The large overlap of the Al trap and the Ta absorber serves to dissipate x-ray induced hotspots. The long qp diffusion length and long electron-phonon scattering time in the Al film[6] contacting the Ta will assist in the removal of hot electrons from the x-ray absorption site. Due to tantalum's short coherence length, only a very small volume of Ta at the Al–Ta interface has reduced gap, and thus the reduced gap Ta proximity layer is rather ineffective in qp trapping. The relatively large trapping volume and small gap of the lateral trap (to the right of the Ta in Figure 1) gives this region the major role in qp trapping. However, the long electron-phonon scattering time in the Al makes even this trapping channel quite slow, approximately 0.1 to 0.5 μs. The Al–Ta interface is of high quality, and will not inhibit qp trapping; measurements of the critical current of simple Ta-Al interfaces have put a lower limit on the current densitiy of the interface at 45,000 A/cm^2. This number is large enough to ensure the bottleneck for qp flow is at the tunnel barrier, as desired.

3. DEVICE CHARACTERISTICS

Current-voltage characteristics of a typical device are given in Figure 2. Traces are obtained in a pumped ^{3}He dewar with a 0.35 K base temperature. These tunnel junctions exhibit very low subgap currents at low voltages, and have sumgaps consistent with very pure Al films. A μ-metal shield is necessary to achieve these low subgap currents; without shielding, currents at $V \approx \Delta/e$ are approximately two times larger, presumably due to trapped flux perpendicular to the junction. A thin film Al meander strip was used in a magnetoresistance measurement to estimate the magnitude of the perpendicular field inside the μ-metal shield. An upper limit (set by the measurement sensitivity) of 0.1 G was found for this field component. For stable current biasing, the Josephson current is suppressed with a parallel magnetic field. We utilize a quartic junction shape to minimize sidelobes in the I_c versus B diffraction pattern.[3,7] As shown in Figure 3, the standard shape has been stretched to maximize the cross-sectional area important for I_c suppression, while keeping the total junction area small for low capacitance and the functional form of the junction edges unchanged. The first zero of I_c with B occurs at about 1 G, consistent with a single flux quantum penetrating the junction. This zero is quite sharp and stable, but due to Fiske modes, we are forced to use approximately 11 G for stable biasing.
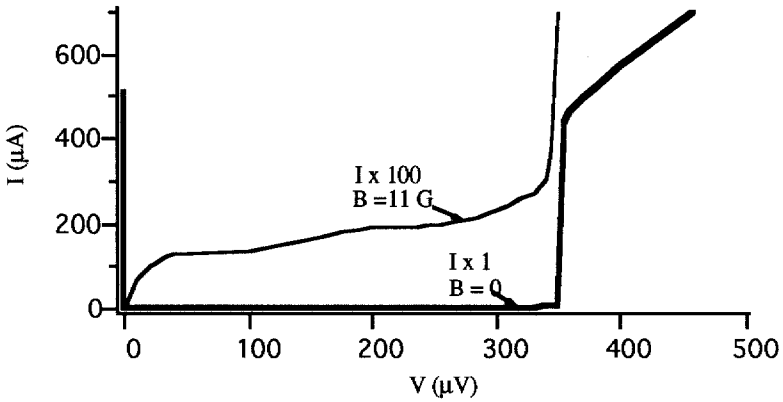
Figure 2: Current-voltage trace of Al-AlOx-Al STJ at T = 0.38 K
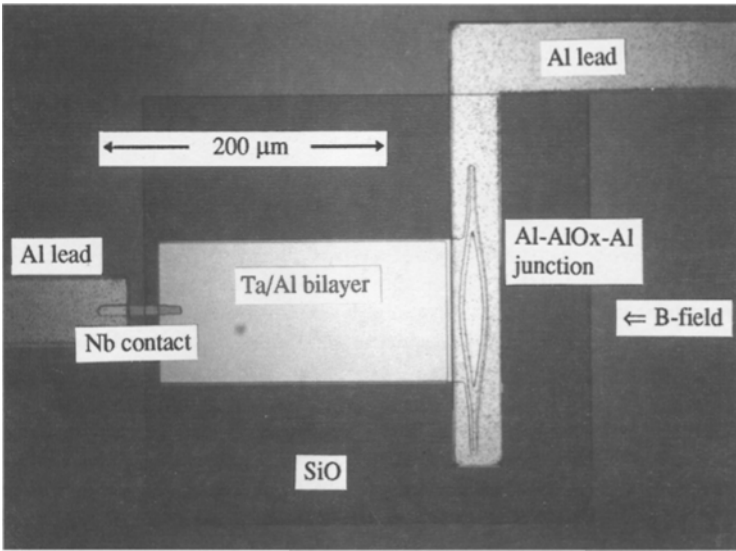
Figure 3: 200x photograph of the device

　　　　Junction normal state resistances of 0.25 to 0.5 ohms ($J_c \approx$ 80 to 40 A/cm^2) are typical with our fabrication process, resulting in a tunneling time of approximately 0.5 to 1 µs. It should be noted that across an entire 2 inch wafer, junction characteristics are quite uniform (<5% variation in R_{nn}), and very stable with time (no change apparent after more than one year stored at room temperature and atmosphere, and after several thermal

cycles). The subgap currents below $V \approx \Delta/e$ are fit well by the BCS theory, indicating our tunnel barriers are of good quality. Subgap current increases with increasing temperature in a BCS fashion, thus giving promise that the currents (and shot noise) will decrease when we use lower temperatures.
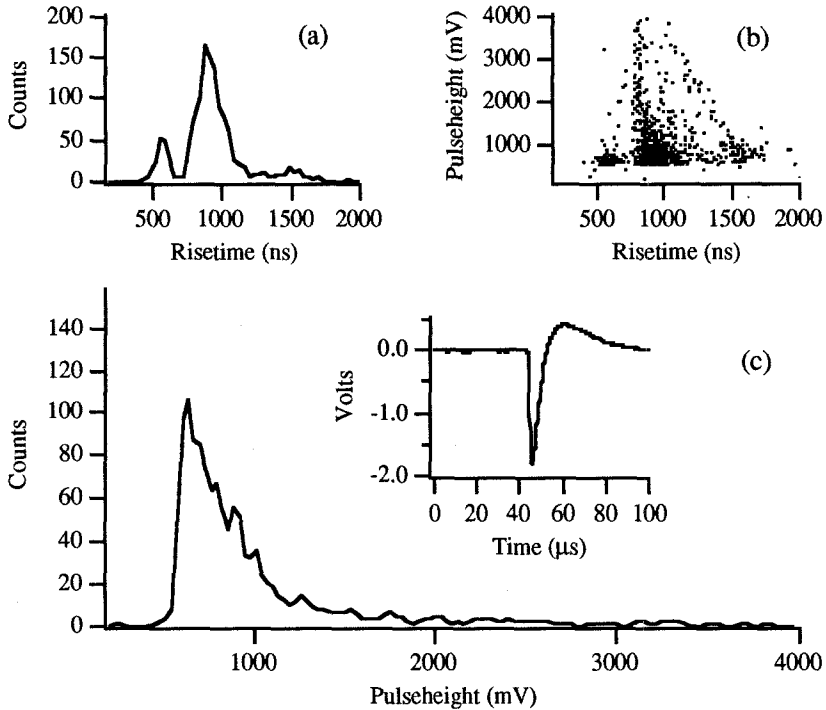
Figure 4: a) Risetime histogram from 5.5 MeV alpha particles, b) Pulseheight vs. risetime, and c)Pulseheight histogram (inset: pulse shape)

4. ALPHA PARTICLE DETECTION

It is generally found that for high resolution x-ray detection, temperatures approaching or below $T_C/10$ are necessary.[2,8] It is therefore not surprising that x-rays are not observed with our devices at a temperature of 0.37 K ($\approx T_C/3$ for the Al junctions). To verify that these devices were indeed suited to detection of an energy deposit, we exposed them to a 5.5 MeV [241]Am alpha particle source. Current pulses resulting from these alpha particles have been observed with signal to noise ratio ≈ 50. A current-sensitive amplifier was used for ease in comparing pulse shapes with theory, and because it is well suited to our low dynamic resistance of ≈ 200 ohms ($R_D/R_{nn} \approx 1000$ at 0.35 K, and increases with temperature even below 0.4 K). We find pulse rise times from film

absorptions of approximately 500 ns, consistent with our diffusion and trapping times. In addition to the thin film absorption events, there is a significantly larger number of substrate events seen by the junctions. These can be differentiated from the film events by their longer risetime (≈ 1 µs) and often greater pulseheight (note that the large majority of alpha particle energy is absorbed by the substrate rather than the thin films[9]). Representative data is shown in Figure 4.

5. DISCUSSION AND CONCLUSIONS

We have demonstrated successful microlithographic fabrication of Nb-Ta-Al-AlOx-Al STJ devices Their design is optimized for STJ x-ray detector operation. They are stable with time and thermal cycling, and have thermally limited subgap current at low voltages.

Alpha particle detection has also been demonstrated. Pulses from the alpha particles show characteristics compatible with expected qp dynamics, but the pulseheights are a factor of ≈ 10 to 100 smaller than expected. This is presumably due to unexpected qp loss, perhaps attributable to inadequate qp lifetime, diffusion length, or trapping rate. In an effort to better understand the loss mechanism, we will perform experiments to determine the qp diffusion length in the films used in our devices.[10]

We are confident that lower temperatures will remedy problems with short qp recombination times and diffusion lengths. Initial tests at lower temperatures will utilize adiabatic magnetization of superconducting zinc and cadmium.[11]   Although this technique does not produce much cooling power, we expect to obtain $T < T_c/6$ long enough to determine the effectiveness of lower temperatures. In the near future we will utilize either a 2-stage ^{3}He, adiabatic demagnetization, or dilution refrigerator.

1 A. Zehnder, C.W. Hagen, and W. Rothmund, SPIE 1344, 286 (1990)

2 H. Kraus *et al.*, Phys. Lett. B 231, 195 (1989)

3 M.C. Gaidis *et al.*, IEEE Trans. Appl. Superconductivity 3, 2088 (1993)

4 N.E. Booth, Appl. Phys. Lett. 50, 293 (1987)

5 D.W. Face, and D.E. Prober, J. Vac. Sci. Tech. A 5, 3408 (1987)

6 K.E. Gray, J. Phys. F: Metal Phys. 1, 290 (1971)

7 E.P. Houwman *et al.*, in Low Temperature Detectors for Neutrinos and Dark Matter IV, N.E. Booth and G.L. Salmon (eds.), Gif-Sur-Yvette Cedex, France: Editions Frontiers, 255 (1992)

8 C.A. Mears *et al.*, submitted to Appl. Phys. Lett., May 1993

9 M. Kurakado, J. Appl. Phys 55, 3185 (1984)

10 S.Y. Hsieh and J.L. Levine, Phys. Rev. Lett. 20, 1502 (1968)

11 M. Yaqub, Cryogenics 1, 101 (1960)